CHEMISTRY
A EUROPEAN JOURNAL

ChemPubSoc
Europe

DOI: 10.1002/chem.201202445

Intrinsically Sulfur- and Nitrogen-Co-doped Carbons from Thiazolium Salts

Jens Peter Paraknowitsch,*[a] Björn Wienert,[a] Yuanjian Zhang,[b] and Arne Thomas[a]

Abstract: Carbon materials that are intrinsically co-doped with nitrogen and sulfur heteroatoms are synthesised by facile annealing of nitrile-functionalised thiazolium salts. Extremely high degrees of doping are achieved, especially for sulfur. The method further allows for direct tuning of the amounts of both N and S, establishing a new synthetic pathway in the emerging field of S-doped carbon materials.

Keywords: carbon · doping · graphite · nitrogen · sulfur

Introduction

Carbonaceous materials doped with heteroatoms have gained major interest in the past years. Besides some examples of boron-doped carbon materials,[1–4] especially nitrogen is a widely studied doping candidate, favourably altering the properties of the respective materials by increasing the overall electron density, especially regarding their electric conductivities and thermal stabilities.[5–9] Different synthetic approaches for the formation of various N-doped carbon materials or composites thereof have been shown; among others the post-functionalization of crude carbons,[10–15] pyrolysis or chemical vapour deposition of N-rich precursors,[16–22] hydrothermal carbonisation of N-rich carbohydrates[23–29] or the use of ionic precursor systems.[30–44] The as-synthesised systems have been further proven to be highly suitable for different fields of application, for example, in supercapacitors,[28,45–47] as electrocatalysts[39–41,48] or for CO_2 capture.[29,36,49] In comparison, sulfur-doped carbon materials are still rare and represent a rather new field within materials sciences. Until less than two years ago, relatively few reports on S-doped carbon could be found; these ranged from graphite–sulfur composites[50,51] to theoretical and fundamental studies on the impact of sulfur atoms in carbon nanotubes or graphene.[52–56] One possible reason for the strong dominance of N doping compared with other heteroatoms might lie in the superior chemical pre-conditions of nitrogen to be incorporated into an aromatic carbon backbone and thus easier synthetic approaches. Nevertheless, in 2011, sulfur has begun to fully enter the spectrum of heteroatom-functionalised carbon materials: microporous sulfur-doped carbon was synthesised from sulfur-rich polymer networks.[57] Furthermore, different routes towards S-doped graphene have been established,[58–60] and most recently, hydrothermal carbonisation routes towards S/N-co-doped carbons have been reported.[61,62] Meanwhile, also the first electrochemical applications of such materials—as electrocatalysts for the reduction of oxygen or as electrodes in supercapacitors—have been realised, which is enabled by the fact that sulfur makes the material more polarisable due to their lone-pair electrons.[58,59,62–64] Considering this effect and further also the preferable influence of nitrogen, it is unbearable that the spectrum of synthetic approaches towards S-doped and S/N-co-doped carbon materials is still tremendously limited. Herein, we are contributing to the hopefully growing toolbox of advanced heteroatom doping, presenting a new synthetic pathway towards S/N-co-doped carbon materials. Ionic liquids (ILs) are used as precursors, as frequently reported for other carbon materials.[30–36,41,42,65–69] ILs functionalised with nitrogen atoms bound into the cationic backbone and nitrile groups exhibit a chemical reactivity that enables carbonisation and subsequent graphitisation, yielding N-doped carbon materials.[30,31,34,35] We synthesised structurally related thiazaolium salts with nitrile functionalities. The presence of sulfur atoms within the cation should alter the carbonisation processes in a way that allows the incorporation of not only N, but also S into the developing carbonaceous material.

Results and Discussion

The two model systems that were used as examples in this study were 3-methyl-thiazol-3-ium-dicyanamide (thia-DCA) and 3-(cyanomethyl)-thiazol-3-ium-bromide (CN-thia). The salts were obtained by quaternisation of the heterocyclic nitrogen atom by using the respective alkyl halide[70] and, in the case of thia-DCA, subsequent anion metathesis[71] (see the Experimental Section for details). The molecular structures and S and N contents are represented in Figure 1. It has to be stated that the presence of two heteroatoms within

[a] Dr. J. P. Paraknowitsch, B. Wienert, Prof. A. Thomas
Berlin Technical University
Institute of Chemistry, Division of Functional Materials
Hardenbergstrasse 40, 10623 Berlin (Germany)
E-mail: jens.p.paraknowitsch@tu-berlin.de

[b] Dr. Y. Zhang
Southeast University
School of Chemistry and Chemical Engineering
Nanjing 211189 (P.R. China)

Supporting information for this article is available on the WWW under http://dx.doi.org/10.1002/chem.201202445.

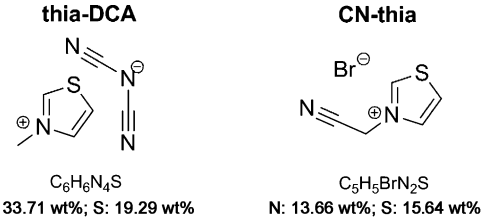

Figure 1. Molecular structures of 3-methyl-thiazol-3-ium-dicyanamide (thia-DCA) and 3-(cyanomethyl)-thiazol-3-ium-bromide (CN-thia).

the cation also decreases the stability of the ring, which coincides with an increased probability of thermal decomposition upon annealing. Nevertheless heating to 500, 600, 700, 800, 900 and 1000 °C under a constant flow of argon did not lead to a complete volatilisation of the precursors, but successfully yielded black solids with a tendency towards highly glossy appearances with increasing temperature. Although the optical appearance of the samples already indicates a graphite-like structure in the resulting material, a more detailed understanding of both elemental composition and structure was attempted with analytical techniques: elemental combustion analysis (EA), powder X-ray diffraction (PXRD) and X-ray photoelectron spectroscopy (XPS).

EA was primarily used to prove the overall suitability of the synthetic concept, because, besides carbon, significant amounts of both nitrogen and sulfur are bound into the structures of the materials; this can be followed in detail in Table 1 and is further illustrated in Figure 2. The change of the elemental compositions of the resulting materials upon increasing the reaction temperature partially occurs in the expected manner. Hydrogen is continuously eliminated; its decreasing amount coincides with the on-going condensation of the material. Carbon contents increase constantly during the carbonisation process. Values of about 85 wt% are reached in the case of both thia-DCA and CN-thia, showing that, although the reactive pathways might slightly differ due to the differences in the compositions of the two ionic compounds, at a certain point the materials equalise and aim at the same target composition. A very similar observation has already been made in previous studies in which purely nitrogen-doped carbons derived from ILs were examined.[30,31] Moreover nitrogen and sulfur contents are constantly decreasing, because the progress of the carbonisation requires the elimination of heteroatoms to enable the formation of a stable carbonaceous backbone. Most interestingly, only in the case of nitrogen, the constant decrease continues up to the highest temperature applied (1000 °C), reaching also very similar contents of 8.75 wt% (thia-DCA) and 7.79 wt% (CN-thia). Also here the similarity is obvious, nonetheless, the slightly higher nitrogen content in the thia-

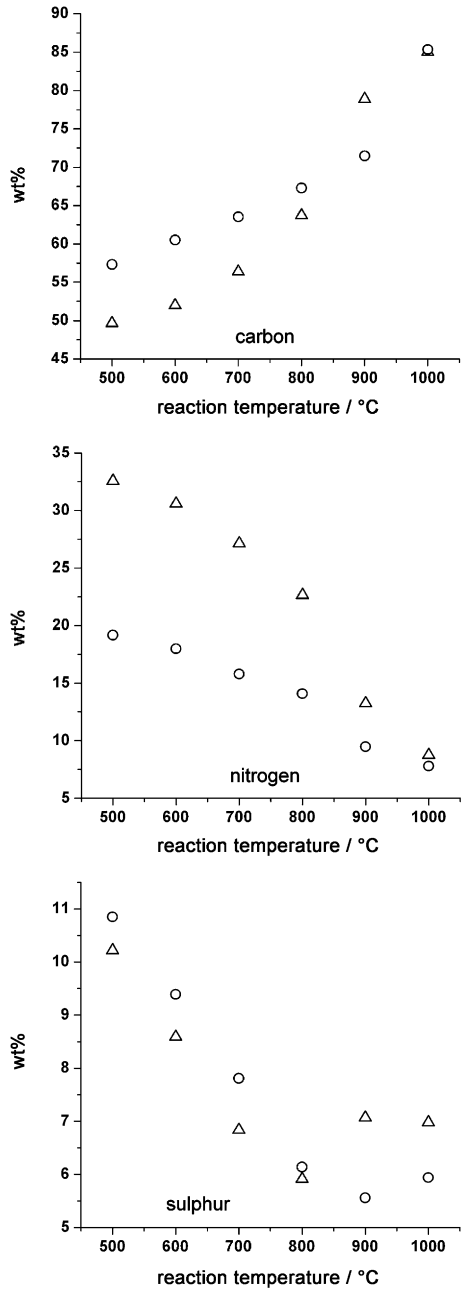

Figure 2. Contents of C, N and S in the resulting materials: △ = thia-DCA, ○ = CN-thia.

Table 1. Contents of C, N, H and S in the target materials determined by EA; in comparison with theoretical values of precursors.

	thia-DCA				CN-thia			
	C [wt%]	N [wt%]	H [wt%]	S [wt%]	C [wt%]	N [wt%]	H [wt%]	S [wt%]
precursor (theory)	43.36	33.71	3.64	19.29	29.28	13.66	2.46	15.64
500 °C	49.66	32.57	2.05	10.22	57.31	19.17	2.23	10.85
600 °C	51.97	30.59	1.90	8.59	60.50	17.98	2.05	9.39
700 °C	56.36	27.14	1.63	6.84	63.52	15.79	1.77	7.81
800 °C	63.71	22.65	1.29	5.91	67.28	14.08	1.67	6.14
900 °C	78.87	13.24	0.85	7.07	71.47	9.47	1.59	5.56
1000 °C	85.02	8.75	0.80	6.98	85.33	7.79	1.12	5.94

DCA-derived material reflects the higher nitrogen content, which is also found in the precursor. Yet sulfur seems to behave chemically differently. A temperature increase from 800 to 900 °C, suddenly increases the sulfur content of the thia-DCA-derived materials, whereas it remains almost the same upon further heating to 1000 °C. Also in the case of CN-thia, an analogous observation can be made, however less pronounced, that is, a temperature increase from 900 to 1000 °C, increases the sulfur content. Also here the resulting materials from both precursors seem to aim at a target content of sulfur, because the values show a clear tendency to equalise. The re-increase of the sulfur content at the highest temperatures applied uncovers additional details about the formation mechanism of the materials. For imidazolium-based precursor systems for merely N-doped carbon materials, the chemical processes are strongly dominated by an elimination of N atoms in form of elemental nitrogen molecules beyond 800 °C, paving the way for the final restructuring necessary for the formation of a graphite-like carbonaceous backbone.[30,31] Most likely, this also occurs upon the thermal treatment of our functional thiazolium precursors, whereas the sulfur atoms already seem to have been incorporated into the forming structure in a far more stable way, which allows them to remain, instead of being eliminated from the material; this leads to an increase of the relative content of sulfur in the material.

EA has thus shown inevitably that S/N-co-doped materials are obtained. The amount of doping can be easily adjusted by choosing the appropriate reaction temperature and the resulting degrees of doping are remarkably high, even at 1000 °C. Such high degrees of doping are highly favourable for material performance and have not yet been achieved by other approaches with low-molecular-weight precursors.[61,62,64] Moreover, it is not only crucial to quantify the elemental composition of the materials, but also to elucidate the chemical environment of the involved elements. Although, in these materials, the potential formation of heteroatom-based surface functionalities or heteroatom moieties that are not bound to carbon are highly unlikely and chemically not comprehensive, it must be proven that sulfur and nitrogen are really incorporated into the carbonaceous backbone. The detailed binding state is also of interest. Therefore, XPS spectra were accomplished for samples synthesised at 600, 800 and 1000 °C. Figure 3 shows the detailed scans of the C1s, N1s and S2p orbitals of the materials synthesised at 1000 °C. All other spectra are represented in Figures S1, S2 and S3 in the Supporting Information. Table 2 sums up the positions of deconvolved peak contributions for all obtained spectra. Regarding nitrogen, in almost all cases (except for thia-DCA at 1000 °C) three contributions are found. The values around 398 eV refer to pyridinic or pyrollic nitrogen species,[64,72] whereas the binding energies around 400 eV can be assigned to quaternary nitrogen bound within a graphite-like framework.[11,64,72,73] This shows that nitrogen is indeed incorporated fully into the carbonaceous material and is not only present as surface functionalities. Moreover an interesting finding lies in the change of intensities between pyridinic/pyrollic moieties and quaternary nitrogen atoms. When the precursors are heated to higher temperatures, more and more nitrogen is firmly bound into

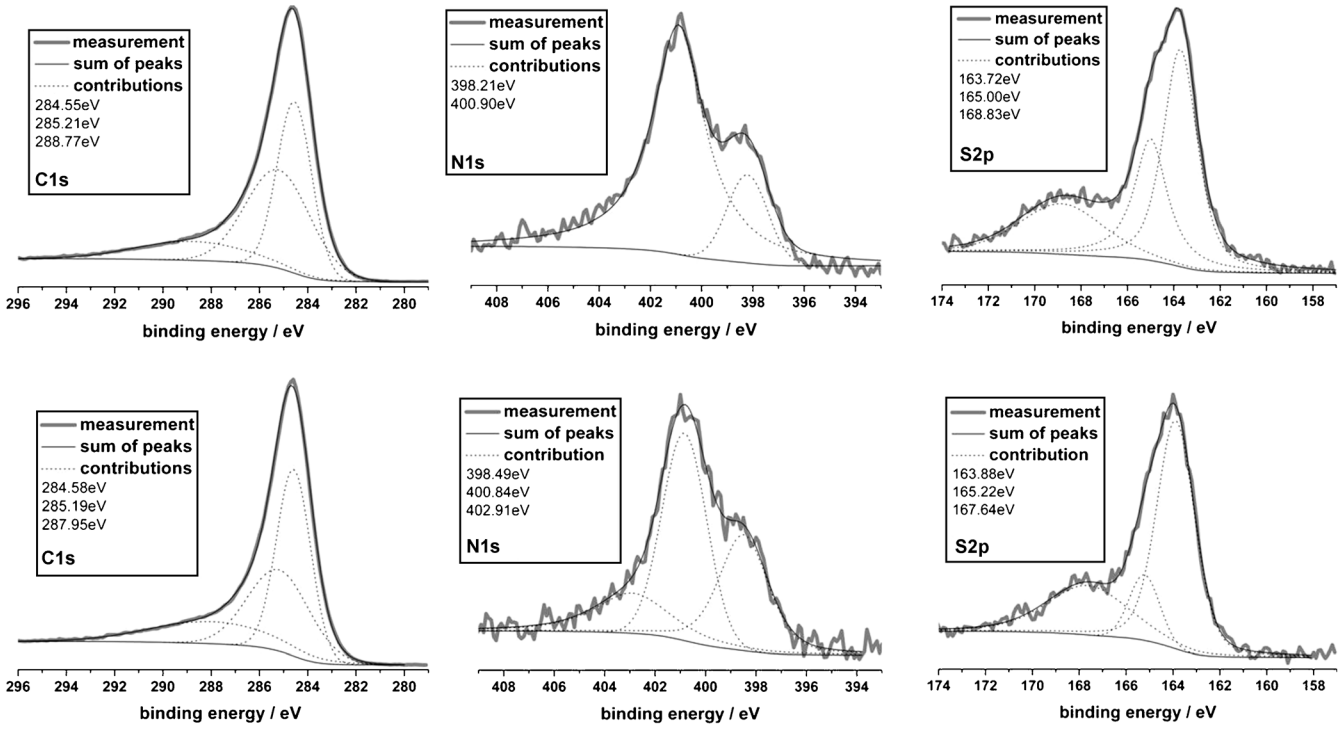

Figure 3. XPS scans for C1s, N1s and S2p orbitals, measured on the materials synthesised at 1000 °C. The upper panel shows spectra of thia-DCA-derived materials and lower panel shows spectra of CN-thia-derived materials.

Table 2. Summary of positions of deconvoluted peaks in the XPS scans of samples synthesised at 600, 800 and 1000 °C from both precursors: * marks the strongest contribution.[a]

	thia-DCA			CN-thia		
	carbon [eV]	nitrogen [eV]	sulfur [eV]	carbon [eV]	nitrogen [eV]	sulfur [eV]
	284.54*	398.19*	163.48*	284.55*	398.19*	163.66*
600 °C	286.07	400.27	164.48	286.18	400.27	164.98
	286.15	403.09	167.90	286.22	403.09	167.95
	284.35*	398.36*	163.58*	284.52*	398.08*	163.61*
800 °C	286.44	400.36	164.89	286.08	400.47*	164.79
	287.45	402.13	166.90	289.29	403.11	167.15
	284.55*	398.21	163.72*	284.58*	398.49	163.88*
1000 °C	285.21	400.90*	165.00	285.19	400.84*	165.22
	288.77	–	168.83	287.95	402.91	167.64

[a] See the Supporting Information for spectra.

the carbon backbone as quaternary graphitic nitrogen; once more, this shows the on-going condensation of the material. Additionally weak contributions are found (except for thia-DCA at 1000 °C) at higher binding energies around 402 or 403 eV. Those can be assigned to oxidised nitrogen species that nonetheless are only of minor intensity and thus minor importance.[64] XPS is a surface method, and carbon materials tend to oxidise slightly at their surfaces, which is represented in this observation. For sulfur a similar situation as that for nitrogen was discovered, as the accordant XPS scans of the S2p orbital are clearly pointing out. In all cases, three contributions are found: the two major contributions appear at approximately 163.5–163.7 eV and 164.5–165 eV. Binding energies around 163.7 eV can refer to C-S-S-C-binding motifs,[74] which are relatively unlikely, because such binding sites might occur preferably between graphitic layers, an energetically unfavourable situation for S-doped materials.[55] However, a special type of sulfur binding was found in the XPS scans of sulfur-doped C_3N_4 at 163.7 eV: replacement of nitrogen atoms by sulfur atoms in triazine units is thus evidenced, which is also in our case a chemically comprehensive explanation of the sulfur-binding environment.[75] The contributions at approximately 164.5–165 eV represent sulfur atoms bound in cyclic carbon structures in an aromatic environment, such as thiophenic sulfur, or C=S double bonds.[74] Thus, also sulfur is primarily bound within the carbon backbone, or attached as C=S at the edges of the backbone. A remarkable difference to the observations for nitrogen is that no crucial changes of intensities of the deconvolved peaks appear. This shows that sulfur atoms are bound in their determined chemical positions already at lower annealing temperatures and that their chemical environments do not change that drastically. This is in perfect agreement with the results of EA, which also indicated such behaviour. In all cases also minor contributions appear at higher binding energies of around 168 eV, referring to oxidised sulfur moieties on the surface of the materials.[74,75] A closer look at the XPS scans of the C1s orbital shows that the most dominant contribution, in all cases around 284.5 eV, comes from aromatic or other sp^2-hybridised carbon atoms bound to neighbouring carbon atoms or hydrogen.[76,77] Additionally slightly less pronounced deconvolved peaks at around 285 or 286 eV refer to electron-poor carbon bound to, for example, nitrogen or sulfur.[64,78,79] Also for carbon, oxidised binding environments represent a minor contribution at high binding-energy values of up to 288 eV.[80] Overall the XPS scans prove that the co-doped carbon materials under discussion consist of a primarily aromatic backbone with the heteroatoms firmly incorporated.

This aromatic binding environment of carbon is of further interest, as it indicates a graphitic structure. The formation of such graphite-like stacking was therefore further investigated by PXRD; the obtained patterns are depicted in Figure 4. All patterns exhibit their most prominent diffraction lines at values of 2θ between 24° and 26°, representing the typical (002) reflex for a graphite-like stacking. This is evidence of a layered motif within the carbonaceous structures, as presumed. Nonetheless, temperatures of 500–1000 °C are obviously not suitable to achieve complete graphitisation of a material, which leads to the pronounced broadening of the diffraction lines. This effect, which shows

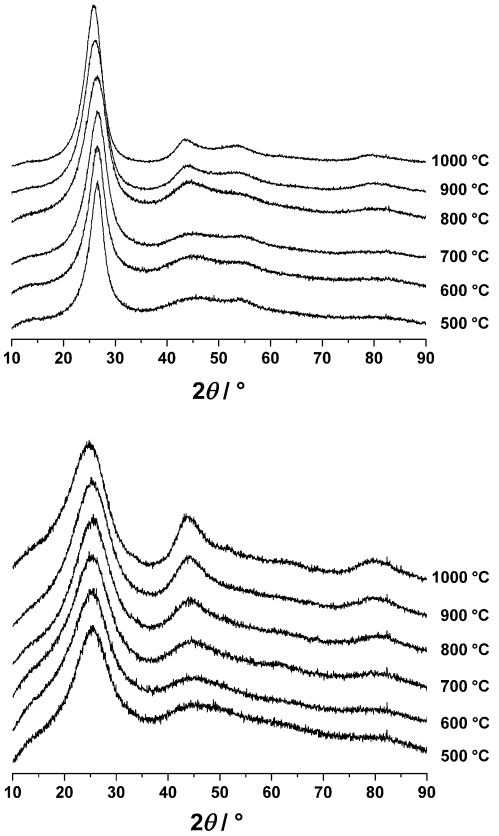

Figure 4. PXRD patterns of thia-DCA-derived materials (top) and CN-thia-derived materials (bottom).

that the stacking is locally limited to only a few nanometres, seems to be stronger for CN-thia-derived materials. One possible reason might lie in the smaller amount of cyano groups in the precursor, yielding less six-membered triazine rings that should ease the formation of honeycomb-shaped carbonaceous layers. Although the materials thus exhibit a rather turbostratic structure, the patterns clearly show the proceeding condensation. In both precursors, the (100) reflexes at angles of $2\theta \cong 43°$ exhibit higher intensities for higher reaction temperatures. This shows that the extension of the layers themselves is increasing and that the overall degree of condensation is thus growing. Also higher-order reflexes with weak intensities appear at angles of $2\theta \cong 80°$. Furthermore a closer look on the (002) diffraction reveals that the high degree of heteroatom doping also alters the microstructure of the graphitic domains. The diffraction line appears at slightly lower values, giving higher interlayer distances than for pure carbon, according to the Bragg equation: For thia-DCA 0.336 nm (500–800 °C), 0.342 nm (900 °C) and 0.345 nm (1000 °C) were calculated. For CN-thia the accordant values are 0.350 nm (500 °C), 0.354 nm (CN-thia, 600–900 °C) and 0.360 nm (1000 °C). This effect is most likely due to stronger electronic repulsion between the layers caused by the increased electron density compared with pure carbon. Yet this effect gets slightly stronger at higher reaction temperatures despite an increase of the C/X ratio (X = heteroatom). As the condensation progress coincides with this phenomenon, the correlations can hardly be securely assigned, but might correlate with the fact that interlayer–intersulfur bonds are not preferred in such structures according to literature.[55]

One disadvantage of the discussed S/N-co-doped carbon materials is the lack of nanostructures or high-active surface areas, caused by missing templating or scaffolding groups or functionalities within the system. Nevertheless it is feasible to induce such high-active surface areas by the simple method of hard templating.[81–83] As a template, Ludox silica nanoparticles with a diameter of 12 nm were used for both precursors at annealing temperatures of 1000 °C. After removal of the template in a hydrofluoric acid bath, the degree of doping of the resulting materials was determined by EA, revealing 6.17 wt % N and 2.17 wt % S for thia-DCA-derived carbon; and 5.19 wt % N and 3.84 wt % S for CN-thia-derived carbon. These slightly lower values than in the bulk material are due to altered reaction mechanisms caused by the enhanced surface area provided by the template. Furthermore the materials were characterised by applying nitrogen sorption and TEM. The isotherms, depicted in Figure 5 A, have been used to determine the surface areas of the template materials by applying the Brunauer–Emmett–Teller (BET) method.[84] High-active surface areas of 1174 $m^2 g^{-1}$ (thia-DCA) and 1195 $m^2 g^{-1}$ (CN-thia) indicate the success of the applied templating method. Furthermore, the shapes of the nitrogen sorption isotherms both exhibit a pronounced hysteresis loops and can thus be classified as type IV or type V isotherms, typical for mesoporous materials. The hysteresis loops are to be classified as type I loops, although the thia-DCA-derived material might rather exhibit a hysteresis-loop shape between types I and II.[85] Hence, a relatively uniformly dispersed pore system is expected; this is in agreement with the Barrett–Joyner–Halenda (BJH)[86] based pore-size distributions, revealing mesopores with pore diameters of approximately 10–12 nm, which also reflects the particles size of the template (see Figure 5 B). Additionally, TEM micrographs (shown in Figure 6) give a conclusive picture of the pore morphology, revealing very open and sponge-like structures of the materials.

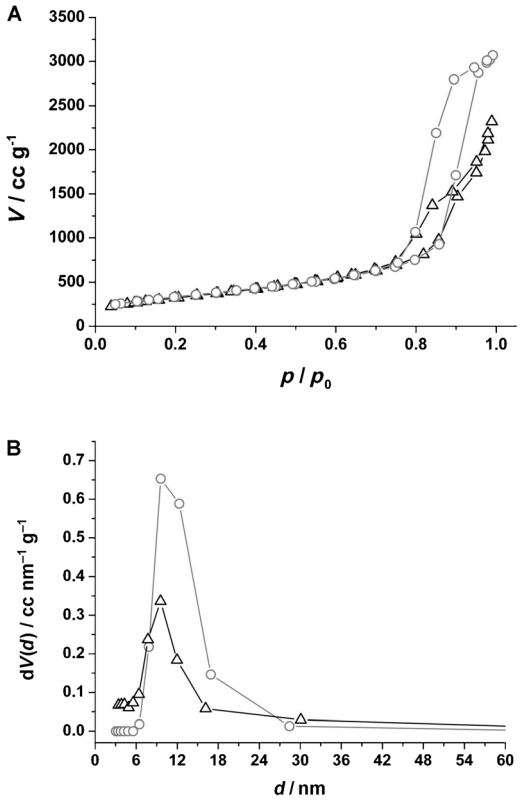

Figure 5. A) Nitrogen sorption isotherms of Ludox templated S/N-co-doped carbons: △ = thia-DCA, 1174 $m^2 g^{-1}$; ○ = CN-thia, 1195 $m^2 g^{-1}$. B) Accordant pore-size distributions, derived from the desorption branch of the isotherms by applying the BJH method: △ = thia-DCA; ○ = CN-thia.

Conclusion

Herein we present a new pathway towards multi-doped carbon materials, carrying both nitrogen and sulfur incorporated into their structures. The use of nitrile-functionalised thiazolium salts as precursors is straightforward, as their mere annealing in an inert-gas atmosphere initiates a carbonisation process that yields S/N-co-doped carbon materials. The degree of doping can simply be tuned by the reaction temperature. The materials exhibit an aromatic graphite-like carbon backbone with remarkably high degrees of heteroatom doping of about 6–8 wt % of both S and N, even

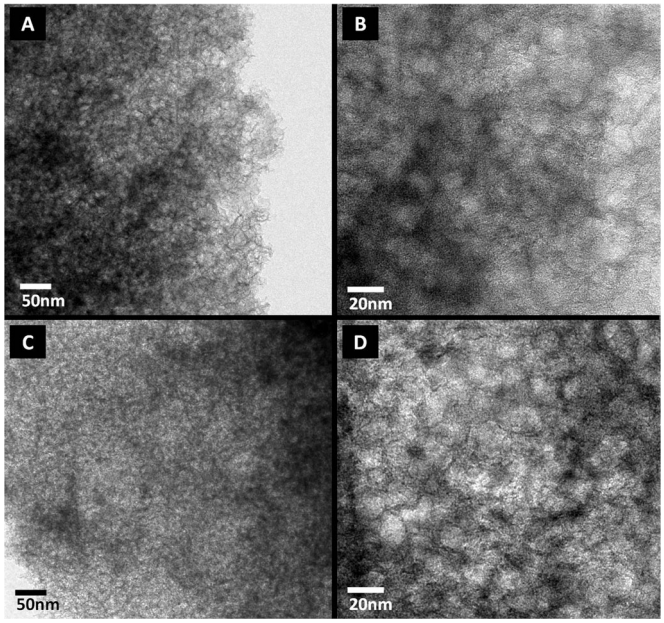

Figure 6. TEM micrographs of Ludox templated S/N-co-doped carbon materials, derived from A, B) thia-DCA and C, D) CN-thia.

at the highest temperature applied (1000 °C). Multiple doping is a promising way for functionalising carbon materials. Nitrogen is already known as a dopant that favourably alters carbon properties, but also sulfur has an outstanding potential in this context. We are therefore currently envisaging the application of the material for electro-catalytical applications, for example, in combination with gold nanoparticles. Thus this work significantly contributes to the emerging field of heteroatom-doped carbon materials that go beyond the widely studied materials merely doped with nitrogen atoms.

Experimental Section

Materials and methods: All reagents were acquired from Sigma Aldrich, exhibiting purities of at least $\geq 97\%$ and used without further treatment. The solvents were also acquired from Sigma Aldrich with a purity of $\geq 99\%$ and used without further treatment. Nitrogen sorption isotherms were measured on a Quadrasorb instrument by Quantachrome, samples were degassed at 120 °C for 20 h under high vacuum before the measurements. X-ray diffraction patterns were measured by using $Cu_{K\alpha}$ radiation on a Bruker D8 Avance powder diffractometer. Transmission electron micrographs were obtained at ZELMI (TU Berlin) from a FEI Tecnai G^2 20 S-TWIN microscope. EA was performed on a Elementar Vario Micro instrument. XPS experiments were performed in type Theta probe (Thermo Fisher) by using monochromatized $Al_{K\alpha}$ radiation at $h\nu =$ 1486.6 eV at NIMS, Japan. Peak positions were internally referenced to the C1s peak at 284.6 eV. Spectra were deconvolved with the XPSPEAK41 software.

Syntheses: Precursor salts were synthesised on the basis of an approach reported in the literature.[70,71] For the formation of thia-DCA, the respective iodide derivative was synthesised in a first step by dissolving thiazole (5 mL, 6 g; 70.5 mmol; 1 equiv) and a high excess of iodomethane (25 mL, 57 g; 401.6 mmol; 5.7 equiv) in methanol (60 mL). The solution was allowed to stir in the dark at room temperature for 24 h. A colourless crystal-like solid precipitated; enhanced precipitation was subsequently achieved by cooling the product solution down in the refrigerator. The solid was separated from the solution by vacuum filtration and subsequently washed with methanol and ethyl acetate to remove iodomethane residues. The product was dried in high vacuum, yielding 3-methyl-thiazol-3-ium-iodide (3.6 g, 15.9 mmol; 23%). EA was used to verify the elemental composition: calcd (wt%): C 21.16, H 2.66, N 6.18, S 14.12; found: C 21.25, H 2.72, N 6.13, S 14.04.

For anion metathesis, 3-methyl-thiazol-3-ium-iodide (3.5 g, 15.4 mmol; 1 equiv) were dissolved in deionised water (100 mL). An excess of silver dicyanamide was prepared by precipitation from aqueous solutions of sodium dicyanamide and silver nitrate. The precipitate was filtered, washed with plenty of deionised water and added to the solution of 3-methyl-thiazol-3-ium-iodide. The colour of the solid changed to yellow immediately, indicating the anion exchange, yielding a solid silver iodide residue. The slurry was allowed to stir overnight in the dark before filtering off the solid. The water was removed with a rotary evaporator under reduced pressure and the yellow-brown product was subsequently dried in vacuo, giving thia-DCA (1.97 g, 11.9 mmol; 77.3%). The product was analysed by EA: calcd (wt%): C 43.36, H 3.64, N 33.71, S 19.29; found: C 42.20, H 3.62, N 31.27, S 18.93.

For the synthesis of CN-thia, thiazole (5 mL, 6 g; 70.5 mmol; 1 equiv) and an excess of 2-bromoacetonitrile (10 mL, 17.7 g; 147.6 mmol; 2.1 equiv) were dissolved in ethyl acetate (100 mL). The solution was allowed to stir for 48 h in the dark. The volume of ethyl acetate was then reduced by 50% with a rotary evaporator and the solution was subsequently refrigerated, leading to the precipitation of colourless crystals. After filtration, the precipitate was washed with ethyl acetate and dried under high vacuum. CN-thia (6.47 g, 31.5 mmol; 44.7%) was obtained. The product was analysed by EA: calcd (wt%): C 29.28, H 2.46, N 13.66, S 15.64; found: C 29.34, H 2.72, N 13.62, S 15.38.

For carbonisation, the respective precursor (500 mg) was placed in a ceramic crucible. Subsequently the samples were annealed in a Nabertherm box-type furnace, equipped with a continuous gas inlet under a constant argon flow of 4 $L\,min^{-1}$ with a heating rate of 100 $K\,h^{-1}$. After the target temperature was reached, the samples were kept at this temperature for 1 h and then allowed to cool down to room temperature. Yields were between approximately 10 and 50%, depending on the temperature used.

Mesoporous S/N-doped carbons were formed by mixing either thia-DCA or CN-thia (600 mg) with water (0.5 mL) before subsequently adding the Ludox silica nanoparticle dispersion (1.4 g) under vigorous stirring. The gel-like mixtures were transferred to ceramic crucibles and heated in a Nabertherm box-type furnace to 1000 °C with a heating ramp of 100 $K\,h^{-1}$ under a constant argon flow of 4 $L\,min^{-1}$. After 1 h at 1000 °C the samples were allowed to cool down. Each product was dispersed in an aqueous solution of ammonium hydrogen fluoride (500 mL, $c = 4$ mol L^{-1}). The mixtures were stirred for 24 h to remove the silica template. After centrifugation, five cycles of washing with deionised water and five cycles of washing with ethanol, the products were dried in a vacuum drying oven at 95 °C.

Acknowledgements

DFG is gratefully acknowledged for funding within the framework of UNICAT cluster of excellence. Dr. Johannes Schmidt is thanked for scientific discussion and support. Further we would like to cordially thank Dr. Caren Göbel for TEM measurements at ZELMI. A very special thanks go to Maria Unterweger, Christina Eichenauer and Anne Sobotta at TU Berlin for their outstanding support of our work.

[1] P. F. Fulvio, J. S. Lee, R. T. Mayes, X. Wang, S. M. Mahurin, S. Dai, *Phys. Chem. Chem. Phys.* **2011**, *13*, 13486.

[2] P. L. Gai, O. Stephan, K. McGuire, A. M. Rao, M. S. Dresselhaus, G. Dresselhaus, C. Colliex, *J. Mater. Chem.* **2004**, *14*, 669.

[3] T. Q. Lin, F. Q. Huang, J. Liang, Y. X. Wang, *Energy Environ. Sci.* **2011**, *4*, 862.
[4] T. Shirasaki, A. Derre, M. Menetrier, A. Tressaud, S. Flandrois, *Carbon* **2000**, *38*, 1461.
[5] Y. Y. Shao, J. H. Sui, G. P. Yin, Y. Z. Gao, *Appl. Catal. B* **2008**, *79*, 89.
[6] H. J. Burch, J. A. Davies, E. Brown, L. Hao, S. A. Contera, N. Grobert, J. F. Ryan, *Appl. Phys. Lett.* **2006**, *89*, 143110.1.
[7] D. Mang, H. P. Boehm, K. Stanczyk, H. Marsh, *Carbon* **1992**, *30*, 391.
[8] Q. H. Yang, W. H. Xu, A. Tomita, T. Kyotani, *Chem. Mater.* **2005**, *17*, 2940.
[9] A. C. M. Carvalho, M. C. dos Santos, *J. Appl. Phys.* **2006**, *100*, 084305.1.
[10] L. Q. Jiang, L. Gao, *Carbon* **2003**, *41*, 2923.
[11] R. Pietrzak, H. Wachowska, P. Nowicki, *Energ. Fuel.* **2006**, *20*, 1275.
[12] S. Glenis, A. J. Nelson, M. M. Labes, *J. Appl. Phys.* **1996**, *80*, 5404.
[13] R. A. Sidik, A. B. Anderson, N. P. Subramanian, S. P. Kumaraguru, B. N. Popov, *J. Phys. Chem. B* **2006**, *110*, 1787.
[14] H. Wang, R. Cote, G. Faubert, D. Guay, J. P. Dodelet, *J. Phys. Chem. B* **1999**, *103*, 2042.
[15] S. C. Roy, A. W. Harding, A. E. Russell, K. M. Thomas, *J. Electrochem. Soc.* **1997**, *144*, 2323.
[16] M. Terrones, P. Redlich, N. Grobert, S. Trasobares, W. K. Hsu, H. Terrones, Y. Q. Zhu, J. P. Hare, C. L. Reeves, A. K. Cheetham, M. Ruhle, H. W. Kroto, D. R. M. Walton, *Adv. Mater.* **1999**, *11*, 655.
[17] M. Terrones, H. Terrones, N. Grobert, W. K. Hsu, Y. Q. Zhu, J. P. Hare, H. W. Kroto, D. R. M. Walton, P. Kohler-Redlich, M. Rühle, J. P. Zhang, A. K. Cheetham, *Appl. Phys. Lett.* **1999**, *75*, 3932.
[18] M. Glerup, M. Castignolles, M. Holzinger, G. Hug, A. Loiseau, P. Bernier, *Chem. Commun.* **2003**, 2542.
[19] M. Terrones, R. Kamalakaran, T. Seeger, M. Ruhle, *Chem. Commun.* **2000**, 2335.
[20] R. Sen, B. C. Satishkumar, S. Govindaraj, K. R. Harikumar, M. K. Renganathan, C. N. R. Rao, *J. Mater. Chem.* **1997**, *7*, 2335.
[21] J. Liu, R. Czerw, D. L. Carroll, *J. Mater. Res.* **2005**, *20*, 538.
[22] R. Gadiou, A. Didion, D. A. Ivanov, I. Czekaj, R. Kötz, C. Vix-Guterl, *J. Phys. Chem. Solids* **2008**, *69*, 1808.
[23] N. Baccile, M. Antonietti, M.-M. Titirici, *ChemSusChem* **2010**, *3*, 246.
[24] R. J. White, M. Antonietti, M.-M. Titirici, *J. Mater. Chem.* **2009**, *19*, 8645.
[25] R. J. White, N. Yoshizawa, M. Antonietti, M.-M. Titirici, *Green Chem.* **2011**, *13*, 2428.
[26] L. Zhao, N. Baccile, S. Gross, Y. Zhang, W. Wei, Y. Sun, M. Antonietti, M.-M. Titirici, *Carbon* **2010**, *48*, 3778.
[27] L. Zhao, R. Crombez, F. P. Caballero, M. Antonietti, J. Texter, M.-M. Titirici, *Polymer* **2010**, *51*, 4540.
[28] L. Zhao, L.-Z. Fan, M.-Q. Zhou, H. Guan, S. Qiao, M. Antonietti, M.-M. Titirici, *Adv. Mater.* **2010**, *22*, 5202.
[29] L. Zhao, Z. Bacsik, N. Hedin, W. Wei, Y. Sun, M. Antonietti, M.-M. Titirici, *ChemSusChem* **2010**, *3*, 840.
[30] J. P. Paraknowitsch, J. Zhang, D. S. Su, A. Thomas, M. Antonietti, *Adv. Mater.* **2010**, *22*, 87.
[31] J. P. Paraknowitsch, A. Thomas, M. Antonietti, *J. Mater. Chem.* **2010**, *20*, 6746.
[32] J. P. Paraknowitsch, Y. J. Zhang, A. Thomas, *J. Mater. Chem.* **2011**, *21*, 15537.
[33] X. Q. Wang, S. Dai, *Angew. Chem.* **2010**, *122*, 6814; *Angew. Chem. Int. Ed.* **2010**, *49*, 6664.
[34] J. S. Lee, X. Q. Wang, H. M. Luo, G. A. Baker, S. Dai, *J. Am. Chem. Soc.* **2009**, *131*, 4596.
[35] J. S. Lee, X. Q. Wang, H. M. Luo, S. Dai, *Adv. Mater.* **2010**, *22*, 1004.
[36] M. C. Gutiérrez, D. Carriazo, C. O. Ania, J. B. Parra, M. Luisa Ferrer, F. del Monte, *Energy Environ. Sci.* **2011**, *4*, 3535.
[37] N. Fechler, T.-P. Fellinger, M. Antonietti, *Chem. Mater.* **2012**, *24*, 713.
[38] T.-P. Fellinger, F. Hasche, P. Strasser, M. Antonietti, *J. Am. Chem. Soc.* **2012**, *134*, 4072.
[39] F. Hasché, T.-P. Fellinger, M. Oezaslan, J. P. Paraknowitsch, M. Antonietti, P. Strasser, *ChemCatChem* **2012**, *4*, 479.
[40] X. Tuaev, J. P. Paraknowitsch, R. Illgen, A. Thomas, P. Strasser, *Phys. Chem. Chem. Phys.* **2012**, *14*, 6444.
[41] W. Yang, T.-P. Fellinger, M. Antonietti, *J. Am. Chem. Soc.* **2011**, *133*, 206.
[42] J. P. Paraknowitsch, A. Thomas, *Macromol. Chem. Phys.* **2012**, *213*, 1132.
[43] T. J. Wooster, K. M. Johanson, K. J. Fraser, D. R. MacFarlane, J. L. Scott, *Green Chem.* **2006**, *8*, 691.
[44] J. P. Paraknowitsch, O. Sukhbat, Y. J. Zhang, A. Thomas, *Eur. J. Inorg. Chem.* **2012**, *26*, 4105.
[45] E. Frackowiak, G. Lota, J. Machnikowski, C. Vix-Guterl, F. Beguin, *Electrochim. Acta* **2006**, *51*, 2209.
[46] G. Lota, B. Grzyb, H. Machnikowska, J. Machnikowski, E. Frackowiak, *Chem. Phys. Lett.* **2005**, *404*, 53.
[47] G. Lota, K. Lota, E. Frackowiak, *Electrochem. Commun.* **2007**, *9*, 1828.
[48] K. Gong, F. Du, Z. Xia, M. Durstock, L. Dai, *Science* **2009**, *323*, 760.
[49] A. Arenillas, T. C. Drage, K. Smith, C. E. Snape, *J. Anal. Appl. Pyrolysis* **2005**, *74*, 298.
[50] R. R. da Silva, J. H. S. Torres, Y. Kopelevich, *Phys. Rev. Lett.* **2001**, *87*, 147001.
[51] E. Z. Kurmaev, A. V. Galakhov, A. Moewes, S. Moehlecke, Y. Kopelevich, *Phys. Rev. B* **2002**, *66*, 193402.
[52] A. Chutia, F. Cimpoesu, H. Tsuboi, A. Miyamoto, *Chem. Phys. Lett.* **2011**, *503*, 91.
[53] P. A. Denis, *J. Phys. Chem. C* **2009**, *113*, 5612.
[54] P. A. Denis, *Chem. Phys. Lett.* **2010**, *492*, 251.
[55] P. A. Denis, *Chem. Phys. Lett.* **2011**, *508*, 95.
[56] P. A. Denis, R. Faccio, A. W. Mombru, *ChemPhysChem* **2009**, *10*, 715.
[57] J. P. Paraknowitsch, A. Thomas, J. Schmidt, *Chem. Commun.* **2011**, *47*, 8283.
[58] Z. Yang, Z. Yao, G. Li, G. Fang, H. Nie, Z. Liu, X. Zhou, X. a. Chen, S. Huang, *ACS Nano* **2012**, *6*, 205.
[59] S. Yang, L. Zhi, K. Tang, X. Feng, J. Maier, K. Müllen, *Adv. Funct. Mater.* **2012**, *22*, 3634.
[60] H. Gao, Z. Liu, L. Song, W. Guo, W. Gao, L. Ci, A. Rao, W. Quan, R. Vajtai, P. M. Ajayan, *Nanotechnology* **2012**, *23*, 275605.
[61] S.-A. Wohlgemuth, F. Vilela, M.-M. Titirici, M. Antonietti, *Green Chem.* **2012**, *14*, 741.
[62] S.-A. Wohlgemuth, R. J. White, M.-G. Willinger, M.-M. Titirici, M. Antonietti, *Green Chem.* **2012**, *14*, 1515.
[63] G. Hasegawa, M. Aoki, K. Kanamori, K. Nakanishi, T. Hanada, K. Tadanaga, *J. Mater. Chem.* **2011**, *21*, 2060.
[64] C. H. Choi, S. H. Park, S. I. Woo, *Green Chem.* **2011**, *13*, 406.
[65] D. Carriazo, M. C. Gutierrez, M. L. Ferrer, F. del Monte, *Chem. Mater.* **2010**, *22*, 6146.
[66] D. Carriazo, F. Pico, M. C. Gutierrez, F. Rubio, J. M. Rojo, F. del Monte, *J. Mater. Chem.* **2010**, *20*, 773.
[67] M. C. Gutiérrez, D. Carriazo, A. Tamayo, R. Jiménez, F. Picó, J. M. Rojo, M. L. Ferrer, F. del Monte, *Chem. Eur. J.* **2011**, *17*, 10533.
[68] M. C. Gutiérrez, F. Rubio, F. del Monte, *Chem. Mater.* **2010**, *22*, 2711.
[69] D. Carriazo, M. C. Serrano, M. C. Gutierrez, M. L. Ferrer, F. del Monte, *Chem. Soc. Rev.* **2012**, *41*, 4996.
[70] A. Kena Diba, C. Noll, M. Richter, M. T. Gieseler, M. Kalesse, *Angew. Chem.* **2010**, *122*, 8545; *Angew. Chem. Int. Ed.* **2010**, *49*, 8367.
[71] D. R. MacFarlane, S. A. Forsyth, J. Golding, G. B. Deacon, *Green Chem.* **2002**, *4*, 444.
[72] P. Burg, P. Fydrych, D. Cagniant, G. Nanse, J. Bimer, A. Jankowska, *Carbon* **2002**, *40*, 1521.
[73] M. C. Huang, H. S. Teng, *Carbon* **2003**, *41*, 951.
[74] B. J. Lindberg, K. Hamrin, G. Johansson, U. Gelius, A. Fahlman, C. Nordling, K. Siegbahn, *Phys. News Phys. Scripta* **1970**, *1*, 286.
[75] G. Liu, P. Niu, C. H. Sun, S. C. Smith, Z. G. Chen, G. Q. Lu, H. M. Cheng, *J. Am. Chem. Soc.* **2010**, *132*, 11642.

[76] XPS Database 20, *Version 3.0*, National Institute of Standards and Technology, Gaithersburg.
[77] J. F. Moulder, W. F. Stickle, P. E. Sobol, K. D. Bomben in *Handbook of X-ray Photoelectron Spectroscopy* (Ed.: J. Chastain), Perkin–Elmer, Eden Prairie, **1992**.
[78] E. T. Kang, K. G. Neoh, K. L. Tan, *Phys. Rev. B* **1991**, *44*, 10461.
[79] C. Silien, M. Buck, G. Goretzki, D. Lahaye, N. R. Champness, T. Weidner, M. Zharnikov, *Langmuir* **2009**, *25*, 959.
[80] M. Sevilla, A. B. Fuertes, *Chem. Eur. J.* **2009**, *15*, 4195.
[81] S. Kubo, R. Demir-Cakan, L. Zhao, R. J. White, M.-M. Titirici, *ChemSusChem* **2010**, *3*, 188.
[82] A.-H. Lu, F. Schueth, *Adv. Mater.* **2006**, *18*, 1793.
[83] A. Thomas, F. Goettmann, M. Antonietti, *Chem. Mater.* **2008**, *20*, 738.
[84] S. Brunauer, P. H. Emmett, E. Teller, *J. Am. Chem. Soc.* **1938**, *60*, 309.
[85] M. Thommes in *Nanoporous Materials: Science and Engineering* (Eds.: G. Q. Lu, X. S. Zhao), Imperial College Press, London, **2004**.
[86] E. P. Barrett, L. G. Joyner, P. P. Halenda, *J. Am. Chem. Soc.* **1951**, *73*, 373.

Received: July 9, 2012
Published online: October 10, 2012

